MARCEL DEKKER, INC. • 270 MADISON AVENUE • NEW YORK, NY 10016

DRUG DEVELOPMENT AND INDUSTRIAL PHARMACY®
Vol. 29, No. 10, pp. 1095–1107, 2003

RESEARCH PAPER

Evaluation of Surface and Bulk Characteristics of Cellulose I Powders in Relation to Compaction Behavior and Tablet Properties

Christina Gustafsson, M.Sc. Pharm., Ph.D. Pharm.,[1,#] Helena Lennholm, Ph.D.,[2] Tommy Iversen, Ph.D.,[3] and Christer Nyström, M.Pharm., Ph.D., M.S.A.P.S.[1,*]

[1]Department of Pharmacy, Uppsala University, Uppsala, Sweden
[2]Department of Pulp and Paper Chemistry and Technology, Division of Wood Chemistry, Royal Institute of Technology, Stockholm, Sweden
[3]Swedish Pulp and Paper Research Institute, Stockholm, Sweden

ABSTRACT

The particle properties and solid-state characteristics of two celluloses, Avicel PH101 and cellulose obtained from the alga *Cladophora* sp., were evaluated and related to the compaction behavior and the properties of the tablets made from them. The surface area of the celluloses was measured at different levels of penetration capacity, ranging from external surface area of particles to molecular texture with Blaine permeametry, Kr-gasadsorption, and solid-state NMR. The important cellulose fibril surface area was best reflected by solid-state NMR, although for the *Cladophora* cellulose, Kr-gas adsorption also resulted in a surface area of the order of what has been suggested earlier on the basis of the cellulose fibril dimensions. The difference in fibril dimension and, thereby, the fibril surface area of the two celluloses was shown to be the primary factor in determining their properties and behavior. Properties such as the crystallinity and the tablet disintegration could be related to the fibril dimensions. The *Cladophora* cellulose resulted in rather strong compacts that still disintegrated rapidly. The irregular surface morphology of the particles and the fragmenting behavior of *Cladophora* probably contributed to the strength of the tablets.

Key Words: MCC; *Cladophora* sp.; Crystallinity; Solid-state NMR; Surface area; Compaction.

[#]Current address: Christina Gustafsson, M.Sc. Pharm., Ph.D. Pharm., Pharmaceutical and Analytical R&D, AstraZeneca R&D Södertälje, Södertälje, Sweden.
*Correspondence: Christer Nyström, M.Pharm., Ph.D., M.S.A.P.S., Department of Pharmacy, Uppsala University, Box 580, SE-751 23 Uppsala, Sweden; Fax: +46-18-471-42-23; E-mail: christer.nystrom@farmaci.uu.se.

DOI: 10.1081/DDC-120025867
0363-9045 (Print); 1520-5762 (Online)

www.dekker.com

1. INTRODUCTION

Microcrystalline cellulose is a commonly used tablet excipient and may act in several ways to improve tableting properties of a formulation used as a filler, a dry binder, or a disintegrant. Microcrystalline cellulose is prepared from wood pulp of high purity consisting mostly of cellulose. Cellulose is a linear polymer composed of β-D-glucosopyranoside units linked by (1–4) bonds. The naturally occurring and most common form of cellulose is called cellulose I. Cellulose I consists in turn of two different allomorphs, cellulose Iα and cellulose Iβ,[1] which differ slightly in their hydrogen-bonding pattern.[2,3] In algae and bacteria, cellulose Iα is the dominant form, whereas cellulose Iβ dominates in higher plants.[1]

The excellent tableting behavior of microcrystalline cellulose has been studied thoroughly over the years and has been explained in terms of its ability to undergo plastic deformation,[4] its relatively high particle surface area,[5,6] and the co-existence of crystalline and disordered structures.[7] Avicel of various grades, originating from wood pulp, has been reported to have a crystallinity of between 55% (measured by solid-state NMR)[8] and 80% (measured by x-ray diffraction).[7] However, a recent NMR study has shown that the true crystallinity of cellulose such as the commercial microcrystalline celluloses may be as low as 10%.[9] Cellulose originating from algae like *Valonia ventricosa* or *Cladophora* sp. has been shown to have a much higher degree of crystallinity (90%–100%) than the commercial microcrystalline celluloses.[8,10] The reason for these differences can be traced to the cellulose fibril dimensions.[11] The cellulose chains in native wood fibers of the cellulose I type are arranged parallel to each other to form fibrils, which in turn aggregate to form fibril aggregates and which in turn form particles (Fig. 1). The number of cellulose chains in the fibrils will differ depending on the source of the cellulose. The width of the cellulose fibrils of wood pulp is approximately 4–5 nm, whereas the corresponding *Cladophora* fibril has been measured to be 13 nm by CP/MAS ^{13}C-NMR,[11] leading to large differences in the fibril surface areas. On the basis of the width of the fibrils and the assumption that the width of a single cellulose chain is 0.55 nm, the surface area of the wood fibril constitutes approximately 47% of the fibril, so the remaining 53% will be the core of the fibril. For a *Cladophora* fibril, only 16% is fibril surface area and the core makes up 84% of the fibril. The surface area of the fibril is disturbed because of contact with other fibril surfaces and is considered to be disordered in contrast to the core or bulk of the fibril, which has a more ordered structure in these materials.[9] Therefore, the ratio of bulk and surface area in a CP/MAS ^{13}C-NMR spectra may be used as a measurement of the crystallinity (i.e., a crystallinity index of the cellulose can be obtained and has been shown to be in good agreement with the calculated values above).[8] Consequently, because celluloses from different sources have different characteristics, it may be expected that they also will differ in terms of their mechanical properties. Thus, properties such as surface areas on different levels and compaction behavior ought to be studied to evaluate important characteristics of the cellulose for the tableting processes.

The aim of this study was to compare and evaluate particle properties and solid-state characteristics of two celluloses: Avicel PH101 representing commercial microcrystalline cellulose and cellulose obtained from the alga *Cladophora* sp. and to relate their properties and characteristics to the compaction behavior and the resulting tablet properties.

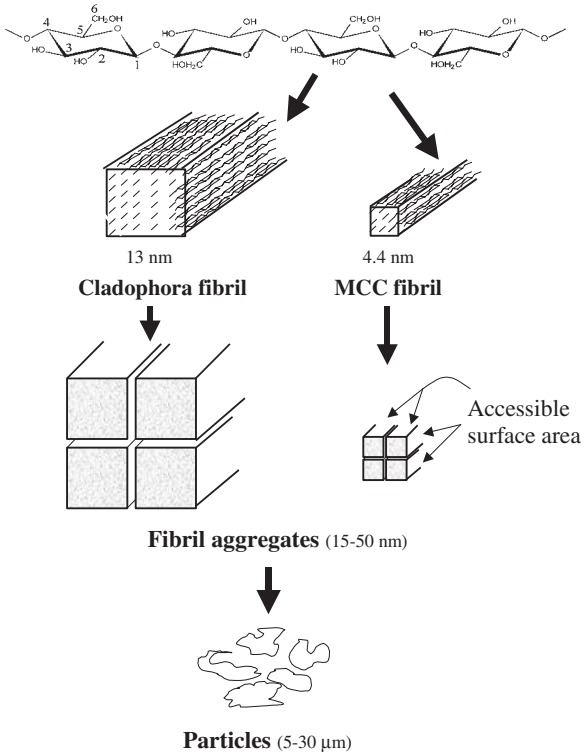

Figure 1. Schematic picture of cellulose at the molecular level, the fibril level, the fibril aggregate level, and the particle level.

2. MATERIALS AND METHODS

2.1. Preparation of Test Materials

Avicel PH 101 (FMC, USA) and cellulose powder prepared from the alga *Cladophora* sp., were studied. The alga *Cladophora* sp. was prepared by hydrolysis and alkaline extraction followed by washing, milling, and spray-drying. The chemical treatment was alternated between acidic hydrolysis (110°C, 3 hr, 1% HCl) and alkaline extraction (110°C, 3 hr, 0.5% NaOH) and repeated. The cellulose was milled in a pin disc mill (Alpine 160 Z, Alpine AG, Germany) and a 5% water suspension of the alga cellulose was spray-dried in a Niro Atomizer (Anhydro, Denmark).

A particle size fraction of 5–30 μm of both Avicel and the *Cladophora* powder was obtained by elutriation by using an air classifier (Alpine 100 MZR, Alpine AG, Germany). The powders prepared were stored at 40% RH and room temperature (22 ± 2°C) before any characterization or compaction was performed.

2.2. Primary Characterization of Test Materials

2.2.1. Surface Texture of Particles

Scanning electron microscopy (LEO 1530, LEO, Germany) was used to characterize the surface texture of the particles.

2.2.2. Particle Density

The apparent particle density[12] was measured by helium pycnometry (Accu Pyc 1330, Micromeretics, USA), ($n = 3$). To obtain the bulk density, the powders were poured into a 25-mL cylinder and weighed ($n = 3$). The tapped density was calculated after tapping the cylinder 1000 times ($n = 3$) in a tap volumeter (Eberhard Bauer D7300, Germany) and the Hausner ratio was calculated from the values of the tapped and bulk density.

2.2.3. Particle Surface Area

Blaine permeametry was used to determine the external surface area of the powders associated with non-porous particles, in accordance with the technique developed by Alderborn et al.[13] The surface area of the powders, including the surface area of all cracks and pores that may be penetrated by the adsorbent, was measured by krypton gas adsorption (ASAP 2000, Micromeretics, USA). The surface area was calculated according to the B.E.T. equation, and the micropore area of the particles was also obtained from these measurements.[14] A qualitative measurement of the surface area on the fibril level was performed by CP/MAS ^{13}C-NMR. The spectrometer (Bruker AMX-300, Germany) operated at 75.47 MHz by using a double air-bearing probe and ZrO_2 rotors. The spinning rate was 5 kHz, the contact time was 0.8 ms, the acquisition time was 37 ms, the sweep width was 368 ppm, and the delay between the pulses was 2.5 sec. For each spectrum, 65,000 transients were accumulated with 2048 data points and zero filled to 4096 data points. The spectra were referenced to the carbonyl in external glycine ($\partial = 176.03$ ppm) and were manually phased.

2.2.4. Particle Size and Shape

Particle size analysis of the test materials was conducted by using laser diffraction analysis (LS 230, Coulter, USA). Because cellulose swells in water, cyclohexane (Extra pure, Merck, Germany) was used as the dispersion medium. The particle shape was determined in terms of the Heywood surface to volume shape factor α_{sv} (calculated as $S_{vp} * d_{sv}$).[15] The volume-specific surface area of the particles, S_{vp}, was obtained from the permeametry measurements and the surface to volume diameter by weight, d_{sv}, was calculated from particle size data obtained from the laser diffraction analysis. However, the geometric mean diameter by volume was used in the calculations instead of the harmonic mean diameter,[16] because of the limitations of the computer program used in this study.

2.2.5. Moisture Content

The moisture content of the powders was determined by a Halogen Moisture Analyzer (HR73, Mettler Toledo, USA) by weighing approximately 1 g of each sample on the moisture balance and heating it at 120°C for 10 min (i.e., the time required to reach a stable plateau where no further

loss was observed in the weight of the powder). The percentage weight loss was then calculated.

2.3. Compression of Powders

The powders were compressed in an instrumented single-punch press (Korsch EK 0, Germany), using flat-faced punches with a diameter of 5.47 mm. These small punches were used to enable intact tablets to be used when conducting solid-state NMR analysis. No lubricant was used. For each compression, 60 mg of powder was weighed on an analytical balance and poured into the die. The maximum upper punch pressure during compression was recorded for each tablet. A deviation from the desired compression load of not more than 5% was accepted. The applied compaction pressures were 10, 20, 50, 100, 200, and 1200 MPa. In addition, the deformability of the powders was characterized by using the Heckel equation.[17,18] The materials were compressed at 150 MPa, and the thickness of the tablets was recorded every millisecond during the compression cycle ($n = 3$). The tablet porosity during the compression cycle was calculated from the thickness of the tablets and was used in the Heckel equation. The yield pressure of the materials was calculated from the reciprocal of the linear part of the Heckel plot, which in this case corresponded to a pressure range of 60–120 MPa. The yield pressure calculated from an in-die Heckel plot is usually considered to reflect the total deformation of the material (i.e., both elastic and plastic deformation)[19,20] and is thus referred to as the apparent yield pressure. The elastic recovery was calculated as the difference between the minimum tablet thickness at 150 MPa compaction load and the maximum tablet thickness after 48 h of storage.[21] After compaction, the tablets were stored at 40% relative humidity and room temperature for at least 48 hr before any characterization was done.

2.4. Characterization of the Compaction Behavior and Tablet Properties

2.4.1. Radial Tensile Strength of the Tablets

The radial tensile strength was calculated by using the diametral compression test.[22,23] The tests were conducted at a speed of 31 mm/min on four tablets from each compaction load (Holland, C50, Great Britain).

2.4.2. Porosity of the Tablets

The apparent particle density of at least 10 tablets from each compaction load was measured by helium pycnometry (Accu Pyc 1330, Micromeretics, USA). The tablet porosity was calculated from the apparent particle density of the tablets and the dimensions and weight of the tablets. The results presented are the average of five tablets.

2.4.3. Surface Area of the Tablets

The external specific surface area of tablets produced with different compaction loads between 0 and 100 MPa was measured by using a Blaine permeameter.[13] The surface area was plotted against the compaction load and the slope of the linear relationship was used as a value of the fragmentation propensity.[13] As for the powders, krypton gas adsorption (ASAP 2000, Micromeritics, USA) was used to measure the surface area including cracks and pores on 2–20 tablets from each compaction load (10–1200 MPa).[14]

2.4.4. Disintegration of Tablets

Disintegration studies were performed on six tablets from each load and for each material in 37°C deionized water (Pharma Test PTZ 1E, Germany) for a maximum monitoring time of 60 min.

2.4.5. Solid-State Characterization of Tablets

To detect changes in the structure of the materials that may have appeared during compression, tablets of each type of cellulose compacted at the maximum compaction load (1200 MPa) were characterized by using CP/MAS ^{13}C-NMR with the same settings as for the powders. The values of the apparent density of the tablets (see Sec. 2.4.2.) were also used for the evaluation of structural change.

3. RESULTS AND DISCUSSION

The complex structure of the cellulose makes it important to define the different structural levels being studied (Figs. 1 and 2). In the following discussion, the smallest structure is the *fibril* (4–20 nm),

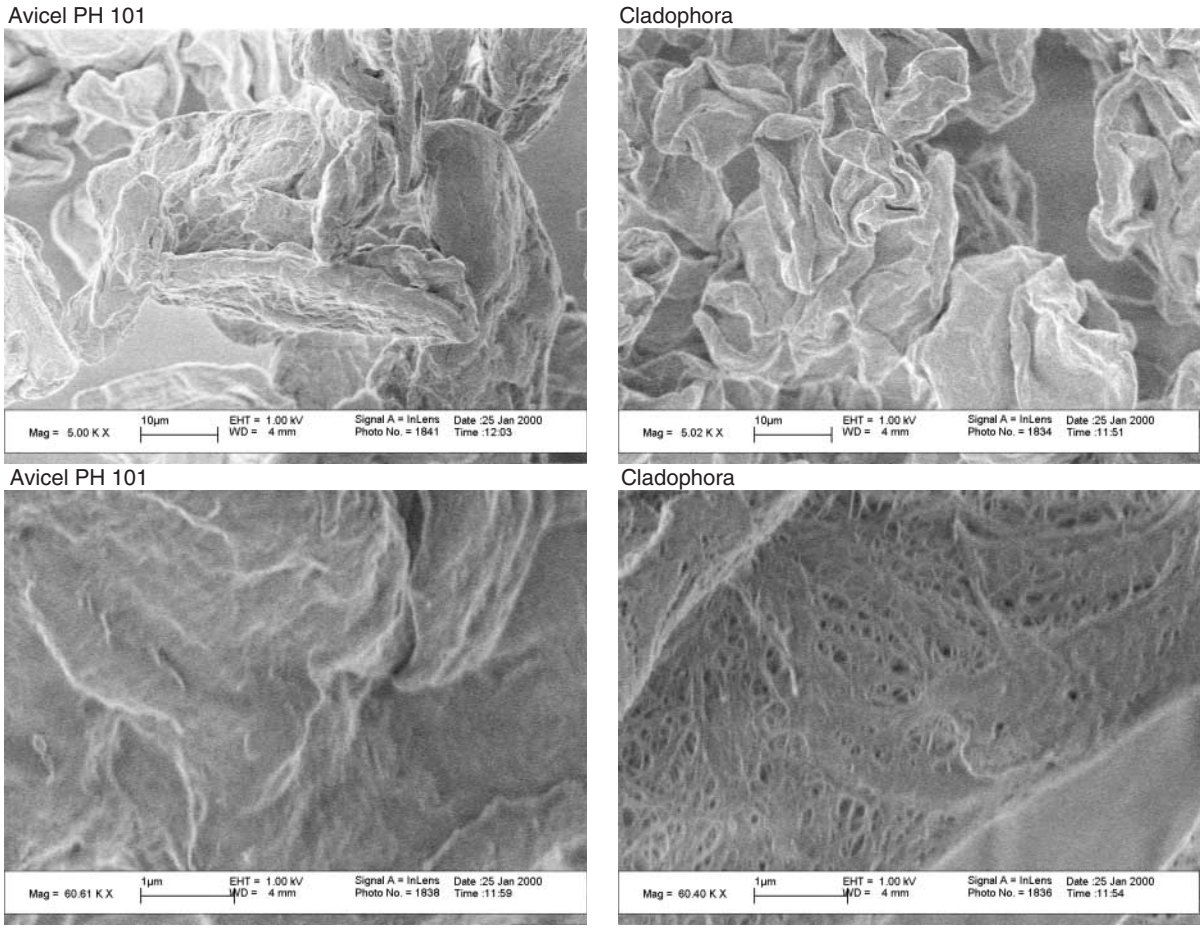

Figure 2. Pictures of the celluloses taken with a scanning electron microscope. The top pictures show the particle structure (bar representing 10 µm), and the bottom ones using a higher magnification (bar representing 1 µm) show the pore structure of the powders.

which makes up *the fibril aggregates* (15–50 nm), which in turn form the *particles* (5–30 µm) of the *powder*. Finally, the powder is compacted to produce *tablets* (mm size).

3.1. Primary Powder Characterization

The apparent particle density, the bulk density, and the tapped density are presented in Table 1 and show considerable differences between the celluloses. The *Cladophora* cellulose had a higher apparent particle density than Avicel PH101, and the opposite was true regarding the bulk and tapped density. Particle size analysis (Fig. 3) revealed differences in the particle size distribution of the powder fractions: Although particle size fractionation had been performed with the intention of obtaining a particle size of 5–30 µm, the eventual particle size range was about 5–100 µm. The *Cladophora* cellulose fraction was shown to consist of smaller particles than the Avicel fraction, which may partly explain the lower bulk and tapped density for the *Cladophora* powder.

The apparent particle density has been shown to reflect the degree of order of a material,[24,25] and in this study, the higher crystallinity of the *Cladophora* powder compared to that of Avicel clearly supports this view. The moisture content of the powders also differed: 5.17% for Avicel and 2.27% for the alga powder. The differences observed are not surprising considering the number of cellulose chains in the fibrils (Fig. 1). Because of the smaller fibril dimension, the Avicel cellulose has a larger proportion of fibril surface area available for water sorption by volume than the *Cladophora* cellulose.[3] The cellulose chains on the surfaces of the fibrils are more mobile

Table 1. Powder characteristics (standard deviations in parentheses, $n = 3$).

	Avicel PH101	*Cladophora*
Apparent particle density (g/cm^3)	1.566 (0.002)	1.612 (0.003)
Bulk density (g/cm^3)	0.335 (0.010)	0.171 (0.002)
Tapped density (g/cm^3)	0.477 (0.008)	0.252 (0.002)
Hausner ratio (–)	1.42	1.47
Moisture content (%)	5.17 (0.08)	2.27 (0.08)
Heywood shape factor (–)	12.5	31

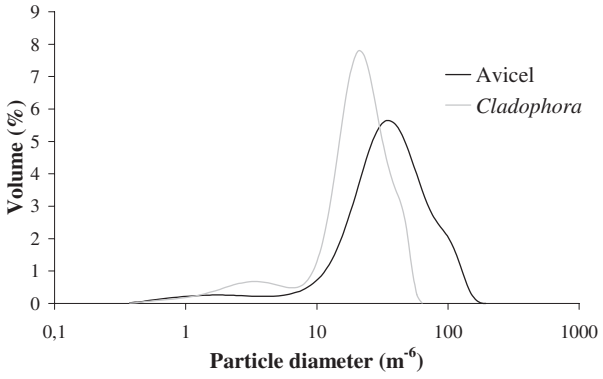

Figure 3. Particle size distribution of Avicel PH101 and *Cladophora* cellulose as measured by laser diffraction.

than the interior of the fibril; a larger fibril surface area will explain the lower crystallinity of the Avicel cellulose compared to the *Cladophora* cellulose. One measure of the crystallinity is given by the so-called crystallinity index (I_{CR}). This is based on the bulk and surface signals of carbon 4 in CP/MAS ^{13}C-NMR spectra. By integration of the surface area under the peak at 86–93 ppm (representing the bulk) and at 80–86 ppm (representing the surface, and in the case of Avicel also small amounts of hemicellulose) the I_{CR} can be calculated and results in a value of 89% for the uncompacted *Cladophora* cellulose and 55% for the Avicel cellulose. These results are in agreement with earlier studies.[8,26] The fibril dimension and, consequently the proportion of fibril surface area in the cellulose are the primary factors determining other properties of the cellulose (such as the crystallinity). Thus, the approach adopted is to discuss the effects of the fibril surface area instead of examining the effect of crystallinity on the different properties of the cellulose, as is usually the case.[7,27]

SEM-pictures of the powders (Fig. 2) showed that the surface morphology of the Avicel particles is more dense than that of the *Cladophora* particles, which instead show a microscopic structure with the appearance of creased paper, containing many folds and pores. The particle shape expressed as the Heywood shape factor was 12.5 and 31 for the Avicel and the *Cladophora* powder, respectively. A high value, such as that obtained for the *Cladophora* powder, is usually connected with shapes like needles and flakes. However, here the folded shape of the *Cladophora* particles probably explains the particle shape factor obtained (Table 1, Fig. 2).

Measurements of the external surface area of the powders by air permeametry revealed a significantly higher surface area for the alga cellulose than of Avicel, 1.7 m^2/g, and 0.4 m^2/g, respectively, as shown in Table 2. However, Kr-gas adsorption analysis showed much larger differences between the materials: for the *Cladophora* cellulose, the specific surface area was 86.6 m^2/g, whereas the Avicel fraction had a surface area of 1.4 m^2/g. The value obtained for Avicel corresponds well to that in the literature,[28–30] and the large differences between the two powders are in agreement with earlier studies.[26,30] The folded particle structure and the open pore system of the *Cladophora* cellulose explain its higher particle surface area (Fig. 2).

Examples of CP/MAS ^{13}C-NMR spectra of the celluloses (Fig. 4) show the six signals from the anhydroglucose unit split into fine structure clusters corresponding to the fibril structure of the cellulose I.[1] The surface area of the fibril aggregates corresponds to the region around 82–86 ppm in the solid-state NMR-spectra (Figs. 4a and b).[11] For the *Cladophora* powder, the peak is very small, indicating that the surface area on this molecular level is low and, as expected, the peak for Avicel in this area is much larger. Thus, the shape of the signal cluster reflects the large differences in the fibril dimensions and the allomorph composition of the celluloses (cellulose Iα and cellulose Iβ).

In a study by Ek et al.,[31] the surface area (S_w) of the elongated fibrils was related to the fibril lateral dimension D and the density ρ according to

$$S_w = \frac{4}{D\rho}$$

From the density data in Table 1 and the gas adsorption data in Table 2, it is possible to calculate the fibril widths of the two celluloses by this equation. These result in a value of 29 nm for the *Cladophora* cellulose and 1.88 μm for the Avicel cellulose. The

value for *Cladophora* is within the range of the fibril aggregate size and is in agreement with previous values obtained,[11,31] suggesting that the Kr gas can reach almost all of the fibril surface area. However, for Avicel, the calculated value differs considerably from the values of around 4 nm for wood cellulose found in the literature.[11] The large value obtained in this study probably partly represents the particle surface and partly the fibril aggregate surface area of Avicel. Because the hydrogen bonding between wood cellulose fibrils is more abundant and the particle structure is tighter than for the *Cladophora* cellulose, the penetration of Kr-gas is partly prohibited.

Table 2. Surface characterization of powders (standard deviations in parenthesis $n = 3$).

	Avicel PH101	*Cladophora*
Specific surface area measured by Blaine permeametry (m^2/g)	0.42 (0.01)	1.72 (0.002)
Specific surface area measured by BET gas-adsorption (Kr) (m^2/g)	1.36 (0.02)	86.65 (0.74)
Micropore area of powder (from pores less than 2 nm) (m^2/g)	0.27 (0.001)	15.50 (0.03)

3.2. Compaction of the Cellulose Powders

3.2.1. Apparent Yield Pressure and Elastic Deformation

Heckel analysis of the celluloses showed a higher average value of apparent yield pressure for the *Cladophora* cellulose (159 MPa) than for the Avicel cellulose (126 MPa). The elastic recovery of Avicel was close to zero, whereas the *Cladophora* cellulose had an elasticity of around 10%. The differences obtained between the two celluloses were not

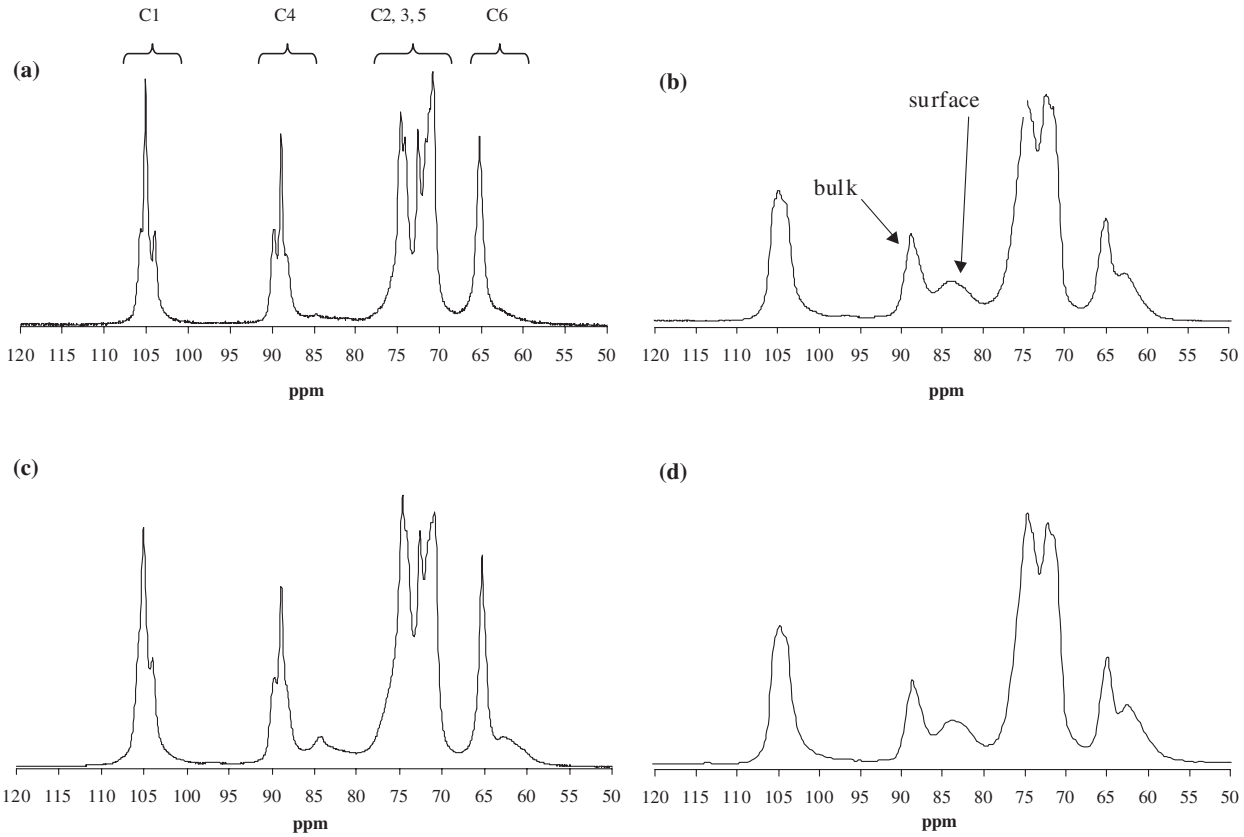

Figure 4. CP/MAS ^{13}C NMR-spectra of (a) a powder sample of *Cladophora* cellulose, (b) a powder sample of Avicel PH101, (c) *Cladophora* tablets compacted at 1200 Mpa, and (d) Avicel PH101 tablets compacted at 1200 MPa. Peak assignments to the anhydroglucose unit are shown in (a); see also Fig. 1.

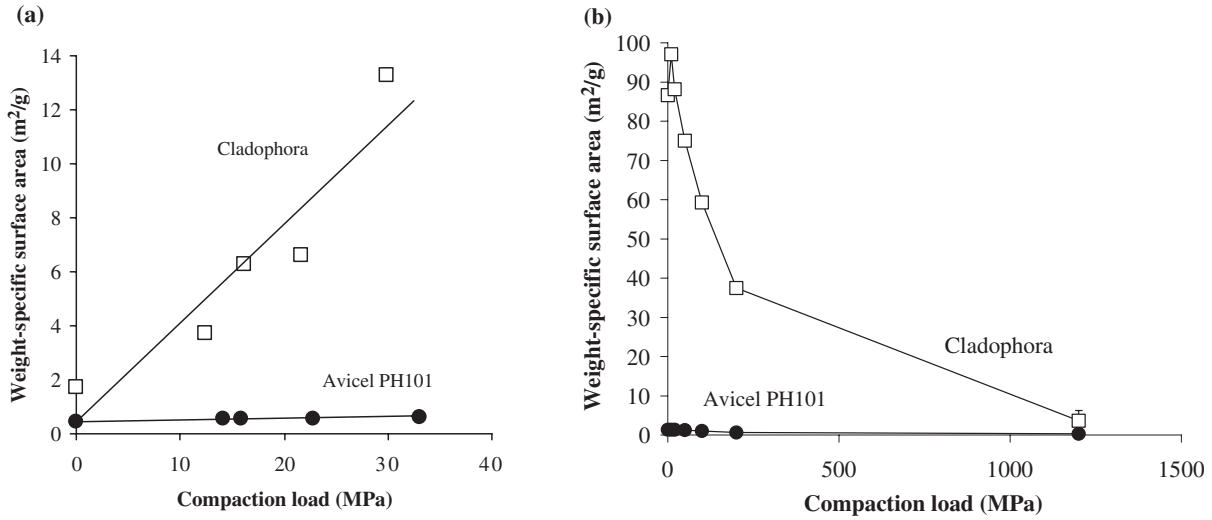

Figure 5. (a) Weight-specific permeametric surface area as a function of the compaction load for Avicel PH101 and *Cladophora* cellulose, (b) weight-specific surface area of Avicel PH101 and *Cladophora* cellulose measured by Kr gas adsorption as a function of compaction load. Standard deviations are shown in (b) ($n \leq 3$).

unexpected because of the larger fibril size of the *Cladophora* cellulose than that of the Avicel cellulose; this possibly results in a more rigid structure that is less prone to undergo plastic deformation. The apparent yield pressure of Avicel PH101 has often been reported to be lower (e.g., Refs.[20,32,33]) and the elasticity higher (e.g., Refs.[33,34] than found in this study. The deviations of our measurements from those in the literature may be caused by the smaller particle size and possibly also partly by the lower compaction pressure and smaller tablet dimensions used in this study for the determination of these values.

3.2.2. Effect of Compaction on Different Levels of Surface Area

The fragmentation propensity, calculated from permeametry data of the compacts (0–100 MPa) of the cellulose powders, differed considerably between the celluloses (Fig. 5a). The *Cladophora* powder showed a fragmentation propensity that is 40 times that of the Avicel powder during compaction. The higher fragmentation propensity of the *Cladophora* powder may probably be explained by its particle structure, which is folded and irregular in comparison to that of the Avicel.

The surface area measured by Kr gas adsorption revealed a strongly decreasing surface area after an initial increase for the *Cladophora* cellulose as the compaction pressure was increased (Fig. 5b). The corresponding surface of Avicel decreased without any initial increase (Fig. 5b). The reason for the decreasing surface area with increasing compaction load may be a reduced ability of the Kr atoms to penetrate the tablets because of the closer and more compact structure created when the powders are compressed. The surface area might also decrease owing to the development of bonds between the surfaces of the particles, although the bonding surface area on the particle level is likely to be small compared to the total surface area.[4,6] In the *Cladophora* cellulose, sealing of the intraparticulate pores due to compaction (Fig. 2b) will probably contribute to a significant decrease of the surface area in absolute terms.[6]

In contrast to the gas adsorption measurements on the particle level, CP/MAS ^{13}C-NMR on tablets compacted at 1200 MPa revealed that there is an increase in the surface area of both the celluloses on the fibril level (Figs. 4c and d). This increased surface area is reflected by the increase in the intensity of the peak around the region of 84–86 ppm for the tablets compared to the uncompacted celluloses (Figs. 4a and b). The compaction will create cracks and dislocations in the interior of fibrils, thereby exposing a larger surface area on the fibril level; the consequence of this will also be a lower value of the crystallinity.[8] The increase in fibril surface area found by solid-state NMR was 180% for *Cladophora* when compacted and 14% for Avicel PH101. The crystallinity index

of both celluloses decreased: for *Cladophora* from 89 to 75% and for Avicel, from 55 to 52%.

Of the three different principles used to measure the surface area in this study, the important fibril surface area is probably best reflected by solid-state NMR, but for the *Cladophora* cellulose, Kr gas adsorption also resulted in a value in agreement with earlier studies of the dimensions of the fibrils.[8,11]

3.3. Tablet Properties

3.3.1. Tablet Tensile Strength

It has been reported that, with its highly ordered structure, crystalline lactose results in low deformability, and consequently, has a low tablet strength compared to a less crystalline form such as spray-dried amorphous lactose.[35] However, compaction of the *Cladophora* cellulose resulted in somewhat stronger tablets in the radial direction than those made of the Avicel cellulose (Fig. 6). Consequently, for the celluloses, the crystallinity does not seem to be a major factor in determining the tablet tensile strength.

The intraparticulate bonding forces in cellulose are hydrogen bonding and van der Waals forces.[36] The bonds created between the particles during compaction are mainly weak distance forces, such as van der Waals forces, but it is likely that hydrogen bonds may also develop and contribute to the interparticulate bond structure.[37] Because of the irregular particle morphology, it has also been suggested that the presence of mechanical interlocking contributes to the tensile strength of microcrystalline cellulose tablets.[38,39]

The higher radial tablet tensile strength obtained for the *Cladophora* tablets may partly be explained by the irregular particle structure of the powder favoring the formation of bonds and particle interaction. Furthermore, the development of new larger particle surfaces due to fragmentation may contribute positively to the tablet tensile strength because these surfaces can be available to some extent for bond formation[40] (Fig. 5a). However, the differences in the magnitude of the surface area values measured by any of the techniques used in this study were much higher than the differences in tablet tensile strength; therefore, it is difficult to estimate the actual bonding surface area and tablet strength from the values obtained for the surface area. It is possible that the higher elasticity of the *Cladophora* cellulose is responsible for breaking interparticulate bonds created during compaction, thus considerably reducing the effective bonding surface area in the final tablet. As a consequence, the tablet tensile strength will not be as high as expected from the surface area measurements.

3.3.2. Porosity

The interparticulate porosity based on the dimensions and the apparent particle density was generally higher for the *Cladophora* tablets than for the corresponding Avicel tablets, except at the highest compaction load (1200 MPa) (see Fig. 7). This is not surprising, considering the higher bulk and tapped

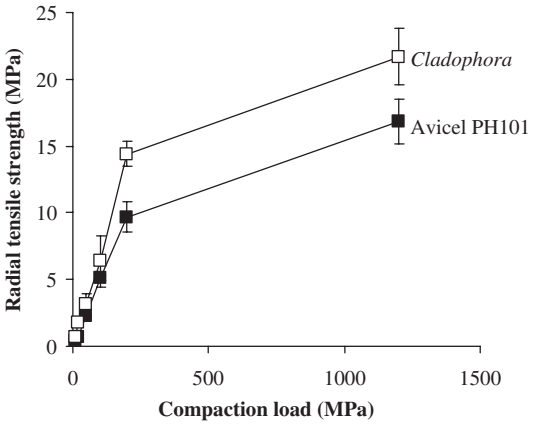

Figure 6. Radial tablet tensile strength as a function of compaction load. Confidence intervals are given for $p = 0.05$.

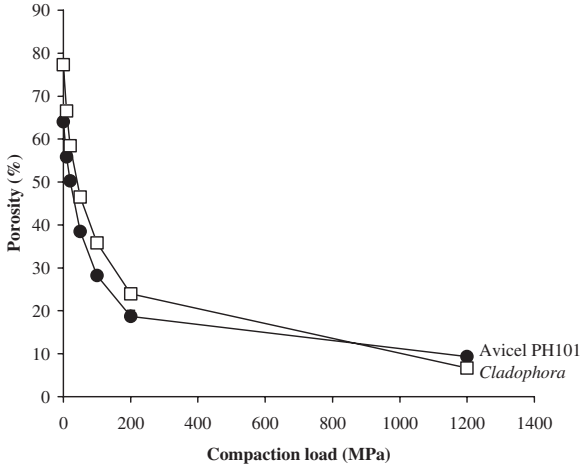

Figure 7. Interparticulate porosity as a function of compaction load, confidence intervals are given for $p = 0.05$.

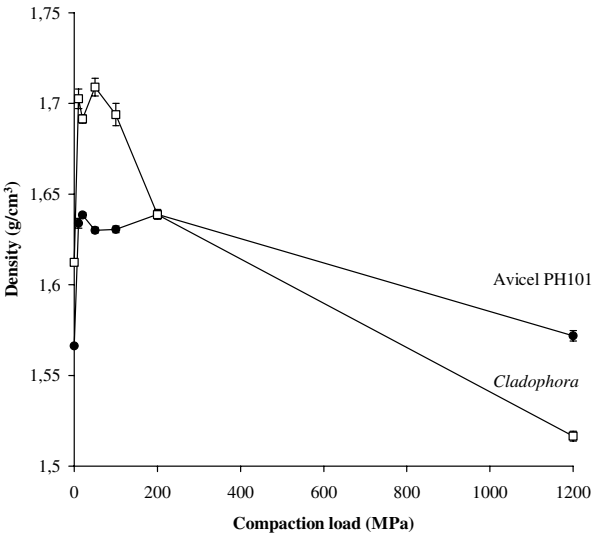

Figure 8. Apparent particle density as a function of compaction load. Error bars represent standard deviations ($n = 30$).

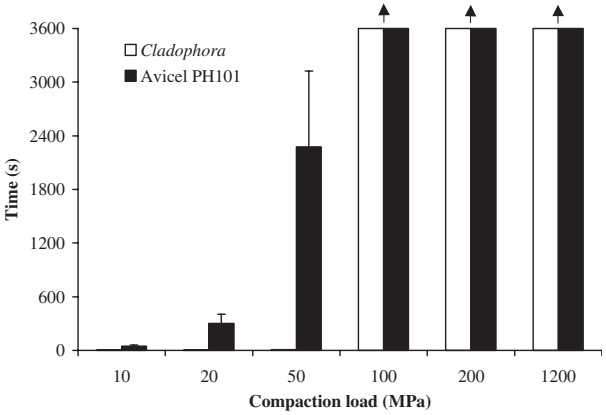

Figure 9. Disintegration of tablets for different compaction loads. Error bars represent standard deviations ($n = 6$) and arrows indicate that the time for disintegration > 60 min.

density of *Cladophora* and the higher resistance to deformation mentioned above (Sec. 3.2). In addition, the higher elasticity of the *Cladophora* will also contribute to the higher porosity of these compacts. The intraparticulate porosity expressed as the micropore area (Table 2) (i.e., the surface area comprised of pores less than 2 nm) obtained from Kr gas adsorption followed the same trend as the interparticulate porosity, being significantly higher for the *Cladophora* cellulose than for the Avicel cellulose. The compaction resulted in a pronounced reduction of the micropore area of the *Cladophora* powder from 15.5 to 2.5 m^2/g, probably caused by sealing of the pores and compaction of the fibril aggregates at high loads.

3.3.4. Density

The changes in apparent particle density of the two powders are presented in Fig. 8. After an initial increase, the density of both powders decreases at very high compaction pressures. The initial increase in density has been reported previously for Avicel PH101,[8,41] and it is thought that it is associated with an increase in order, probably rising from the removal of internal distortions in the interior of the fibril aggregates at moderate compaction loads. The phenomenon has also been reported for acetylsalicylic acid[42] and polyethylene glycol.[43] However, too high loads will destroy the order by creating new dislocations, and consequently, cause a decrease in order.[8] The destructive effect was most pronounced for the *Cladophora* cellulose (Fig. 8). This may probably be explained in terms of the differences in distorted cellulose chains in the fibrils as discussed above (Sec. 3.1.).

3.3.5. Disintegration of Tablets

Although the *Cladophora* compacts had a slightly higher tensile strength than the Avicel compacts, the disintegration of *Cladophora* compacts at compaction loads below 100 MPa was very much faster than for the corresponding Avicel compacts (Fig. 9). Even at higher loads, the *Cladophora* compacts showed a higher degree of disintegration after 1 hr (when the experiment was stopped) than the Avicel compacts. The absolute moisture content of the *Cladophora* cellulose was only half that of the Avicel and therefore, would not favor the fast disintegration. On the other hand, as mentioned in the introduction, for a *Cladophora* fibril, only 16% is fibril surface area and calculating the moisture content per (surface area) square measure available on the fibril level results in a much higher value for the *Cladophora* cellulose, in agreement with the faster disintegration. However, the higher intra- and interparticulate porosity of these tablets and the fewer amount of hydrogen bonds in the *Cladophora* fibril aggregates and particles to be broken in contact with water will probably be the most important factors favoring a faster disintegration (Fig. 7).

4. CONCLUSIONS

This study shows that the difference in fibril dimension and, thereby, the fibril surface area of the two celluloses Avicel PH101 and *Cladophora* cellulose is a primary factor responsible for some of their properties and behavior. Properties such as the density and the crystallinity will be strongly affected by the size of the fibril. The *Cladophora* cellulose resulted in rather strong compacts that still disintegrated rapidly. The irregular surface morphology of the particles and the fragmenting behavior of *Cladophora* probably contributed to the strength of the tablets. At the same time, the larger fibril dimension resulted in less hydrogen bonding between the fibril aggregates and a higher moisture content per square measure on the fibril level than Avicel PH101, favoring a faster disintegration of *Cladophora* tablets at moderate compaction loads.

Of the three different principles used to measure the surface area in this study, permeametry, Kr-gas adsorption, and solid-state NMR, the fibril surface area was best reflected by CP/MAS ^{13}C-NMR, and for the *Cladophora* cellulose, Kr-gas adsorption also resulted in a surface area in the order of what was previously reported on the basis of the fibril width.

ACKNOWLEDGMENTS

The authors thank Dr. Tomas Larsson, Swedish Pulp and Paper Research Institute, STFI, for valuable comments and help in relation to the solid-state NMR spectra and Dr. Ragnar Ek, Department of Pharmacy, Uppsala University, for generously contributing with samples of *Cladophora* alga. AstraZeneca (Sweden), Pharmacia (Sweden) and the Knut and Alice Wallenberg Foundation are gratefully acknowledged for financial support.

REFERENCES

1. VanderHart, D.L.; Atalla, R.H. Studies of microstructure in native celluloses using solid-state ^{13}C-NMR. Macromolecules **1984**, *17*, 1465–1472.
2. Sugiama, J.; Persson, J.; Chanzy, H. Combined infrared and electron diffraction study of the polymorphism of native celluloses. Macromolecules **1991**, *24*, 2461–2466.
3. Heiner, A.P.; Kuutti, L.; Teleman, O. Comparison of the interface between water and four surfaces of native crystalline cellulose by molecular dynamics simulations. Carbohydr. Res. **1998**, *306*, 205–220.
4. Sixsmith, D. The effect of compression on some physical properties of microcrystalline cellulose. J. Pharm. Pharmacol. **1976**, *29*, 33–36.
5. Nyström, C.; Alderborn, G.; Duberg, M.; Karehill, P.G. Bonding surface area and bonding mechanism—two important factors for the understanding of powder compactability. Drug Dev. Ind. Pharm. **1993**, *19*, 2143–2196.
6. Nyström, C.; Karehill, P.G. Studies on direct compression of tablets XVI. The use of surface area measurements for the evaluation of bonding surface area in compressed powders. Powder Technol. **1986**, *47*, 201–209.
7. Doelker, E.; Gurny, R.; Schurz, J.; Janosi, A.; Matin, N. Degrees of crystallinity and polymerization of modified cellulose powders for direct tabletting. Powder Technol. **1987**, *52*, 207–213.
8. Ek, R.; Wormald, P.; Östelius, J.; Iversen, T.; Nyström, C. Crystallinity index of microcrystalline cellulose particles during compression of tablets. Int. J. Pharm. **1995**, *125*, 257–264.
9. Larsson, P.T.; Wickholm, K.; Iversen, T. A CP/MAS 13C NMR investigation of molecular ordering in celluloses. Carbohydrate Res. **1997**, *302*, 19–25.
10. Isogai. Allomorphs of cellulose and other polysaccharides. In *Cellulosic Polymers—Blends and Composites*; Gilbert, R.D., Ed.; Carl Hanser Verlag: München, 1994; 1–24.
11. Wickholm, K.; Larsson, P.T.; Iversen, T. Assignment of noncrystalline forms in cellulose I by CP/MAS ^{13}C NMR spectroscopy. Carbohydr. Res. **1998**, *312*, 123–129.
12. British Standard 12. Glossary of terms relating to powders, no. 505, British Standard Institute, Park Street, London, UK, 1958.
13. Alderborn, G.; Duberg, M.; Nyström, C. Studies on direct compression of tablets X. Measurement of tablet surface area by permeametry. Powder Technol. **1985**, *41*, 49–56.
14. Webb, P.A.; Orr, C. Analytical methods in fine particle technology. Micromeritics Instrument Corp. Norcross, USA **1997**, 53–153.
15. Heywood, H. Particle shape coefficient. J. Imp. Coll. Chem. Eng. Soc. **1954**, *8*, 25–33.
16. Herdan, G. *Small Particle Statistics*, 2nd Ed.; Pitman Press: Bath, 1960; 35 p.
17. Heckel, R.W. Density-pressure relationships in powder compaction. Trans. Metall. Soc. Aime **1961**, *221*, 671–675.

18. Heckel, R.W. An analysis of powder compaction phenomena. Trans. Metall. Soc. Aime **1961**, *221*, 1001–1008.
19. Duberg, M.; Nyström, C. Studies on direct compression of tablets. XVII. Porosity-pressure curves for the characterization of volume reduction mechanisms in powder compression. Powder Technol. **1986**, *46*, 67–75.
20. Paronen, P. Heckel plots as indicators of elastic properties of pharmaceuticals. Drug Dev. Ind. Pharm. **1986**, *12*, 1903–1912.
21. Armstrong, N.A.; Haines-Nutt, R.F. Elastic recovery and surface area changes in compacted powder systems. J. Pharm. Pharmacol. **1972**, *24*, 135P.
22. Nyström, C.; Malmqvist, K.; Mazur, J.; Alex, W.; Hölzer, A.W. Measurement of axial and radial strength of tablets and their relation to capping. Acta Pharm., Suec. **1978**, *15*, 226–232.
23. Fell, J.T.; Newton, J.M. Determination of tablet strength by the diametral compression test. J. Pharm. Sci. **1970**, *59*, 688–691.
24. Hüttenrauch, R.; Fricke, S.; Zielke, P. Mechanical activation of pharmaceutical systems. Pharm. Res. **1985**, *2*, 302–306.
25. Suryanarayanan, R.; Mitchell, A.G. Evaluation of two concepts of crystallinity using calcium gluceptate as a model compound. Int. J. Pharm. **1985**, *24*, 1–17.
26. Gustafsson, C.; Nyström, C. *Different Principles in Measuring Surface Area of Cellulose Powders*; Läkemedelskongressen, Älvsjö: Sweden, October 19–21, 1998; 125 p.
27. Dittgen, M.; Fricke, S.; Gerecke, H. Microcrystalline cellulose in direct tableting. Manuf. Chemist. **1993**, *64*, 17–21.
28. Adolfsson, Å.; Gustafsson, C.; Nyström, C. Use of tablet strength adjusted for surface area and mean interparticulate distance to evaluate dominating bonding mechanisms. Drug Dev. Ind. Pharm. **1999**, *25* (6), 753–764.
29. Nakai, Y.; Fukuoka, E.; Najkajima, S.; Hasegawa, J. Crystallinity and Physical characteristics of microcrystalline cellulose. Chem. Pharm. Bull. **1977**, *25* (1), 96–101.
30. Zografi, G.; Kontny, M.J.; Yang, A.Y.S.; Brenner, G.S. Surface area and water vapor sorption of microcrystalline cellulose. Int. J. Pharm. **1984**, *18*, 99–116.
31. Ek, R.; Gustafsson, C.; Nutt, A.; Iversen, T; Nyström, C. Cellulose powder from *Cladophora* sp. algae. J. Molecular Recognition **1998**, *11*, 263–265.
32. Roberts, R.J.; Rowe, R.C. The effect of the relationship between punsch velocity and particle size on the compaction behavior of materials with varying deformation mechanics. J. Pharm. Pharmacol. **1986**, *38*, 567–571.
33. Doelker, E. Comparative compaction properties of various microcrystalline cellulose types and generic products. Drug Dev. Ind. Pharm. **1993**, *19*, 2399–2471.
34. Mattsson, S.; Nyström, C. Evaluation of strength-enhancing factors of a ductile binder in direct compression of sodium bicarbonate and calcium carbonate powders. Eur. J. Pharm. Sci. **2000**, *10*, 53–66.
35. Sebhatu, T.; Alderborn, G. Relationships between the effective interparticulate contact area and the tensile strength of tablets of amorphous and crystalline lactose of varying particle size. Eur. J. Pharm. Sci. **1999**, *8*, 235–242.
36. Cousins, S.K.; Brown, R.M. Cellulose I microfibril assembly: computational molecular mechanics energy analysis favors bonding by van der Waals forces as the initial step in crystallization. Polymer **1995**, *36*, 3885–3888.
37. Nyström, C.; Karehill, P.G. The importance of intermolecular bonding forces and the concept of bonding surface area. In *Pharmaceutical Powder Compaction Technology*; Alderborn, G., Nyström, C., Eds.; Marcel Dekker, Inc.: New York, 1996; 22.
38. Karehill, P.G.; Glazer, M.; Nyström, C. Studies on the direct compression of tablets XXII. The importance of surface roughness for the compactability of some directly compressible materials with different bonding mechanisms and volume reduction properties. Int. J. Pharm. **1990**, *64*, 35–43.
39. Adolfsson, Å.; Olsson, H.; Nyström, C. Effect of particle size and compaction load in interparticulate bonding structure for some pharmaceutical materials studied by compaction and strength characterization in butanol. Eur. J. Pharm. Biopharm. **1997**, *44*, 243–251.
40. Nyström, C.; Karehill, P.G. The importance of intermolecular bonding forces and the concept of bonding surface area. In *Pharmaceutical Powder Compaction Technology*; Alderborn, G., Nyström, C., Eds.; Marcel Dekker, Inc.: New York, 1996; 44–51.

41. Kumar, V.; Kothari, S.H. Effect of compressional force on the crystallinity of directly compressible cellulose excipients. Int. J. Pharm. **1999**, *177*, 173–182.
42. Pedersen, S.; Kristensen, H.G. Change in crystal density of acetylsalicylic acid during compaction. S.T.P Pharm. Sci. **1994**, *4*, 201–206.
43. Adolfsson, Å.; Nyström, C. Tablet strength, porosity, elasticity, and solid state structure of tablets compressed at high loads. Int. J. Pharm. **1996**, *143*, 95–106.